**Supporting information**

# Study on the zinc porphyrins as potential carbonic anhydrase mimics for promoting $CO_2$ absorption in $K_2CO_3$ solution

Yuchen Zhou[a], Zezhi Chen [a*], Huijuan Gong[a,b*], Xiaoshu Wang[b], Lu Chen[b], Huiqiang Yu[b]

[a]State Key Laboratory of Pollution Control and Resource Reuse, School of Environment, Nanjing University, Nanjing, 210023, PR China

[b]Center of Materials Analysis, Nanjing University, 210093, Nanjing, PR China

*Corresponding authors.

E-mail addresses: chenzzg@nju.edu.cn (Z. Chen), gonghj@nju.edu.cn (H. Gong).

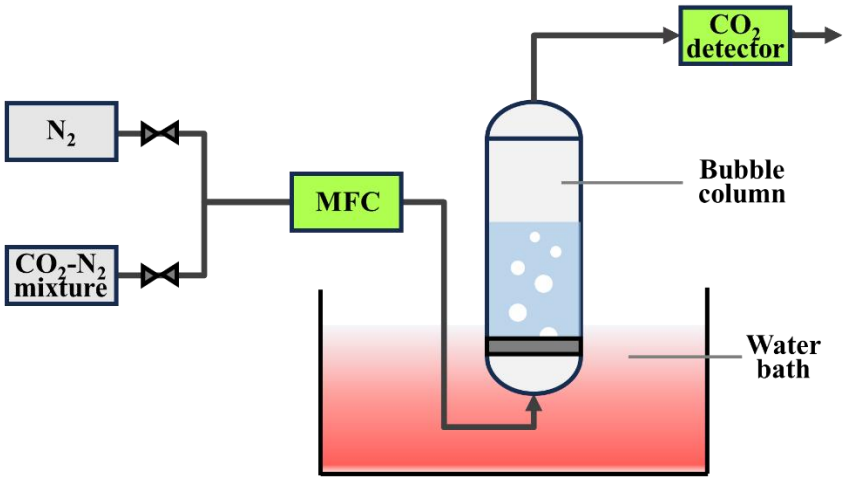


**Supplementary Fig. 1| Schematic diagram of the experimental setup for $CO_2$ absorption and regeneration.**

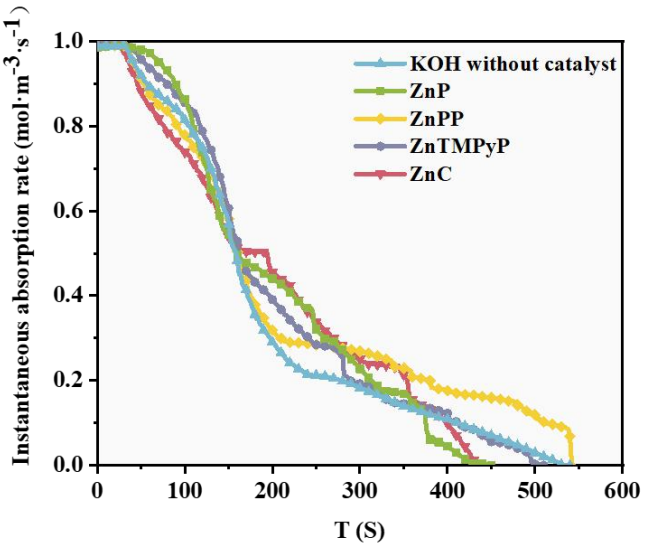


**Supplementary Fig. 2| Instantaneous $CO_2$ absorption rate curves of $K_2CO_3$ solutions with different catalysts at first round.** Absorption conditions—Total volume of absorbent: 30 mL; $K_2CO_3$ concentration in solutions: 2 wt.%; temperature: 30 ℃; absorption time: 550 s; total gas flow rate: 400 mL/min; gas composition: $CO_2/N_2$ mixture (10/90, vol/vol.).

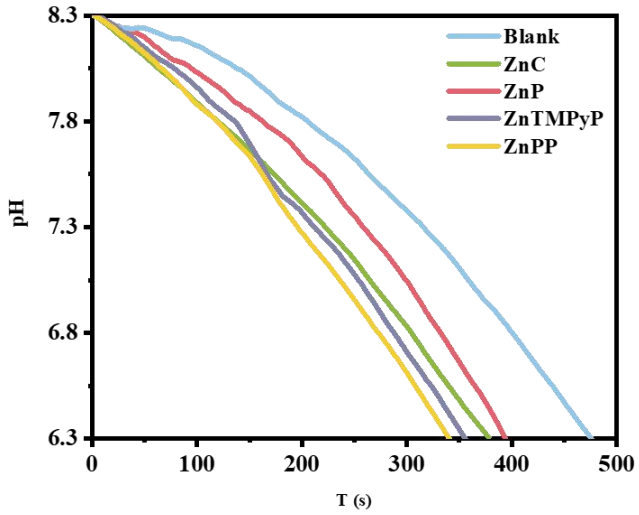


**Supplementary Fig. 3**| The pH change curve of each reaction solution over time.

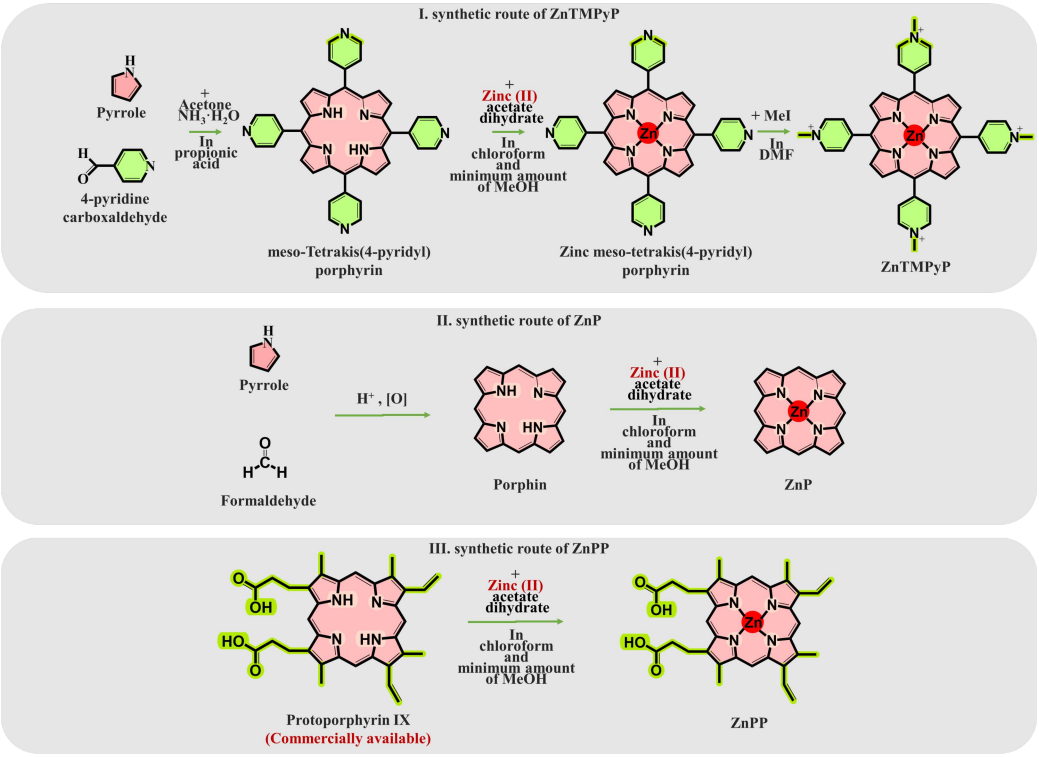


**Supplementary Fig. 4**| Synthetic routes of catalysts.

**Supplementary Table 1.** The Average $CO_2$ Absorption Rate ($\bar{R}$), $CO_2$ Absorption Amount (m), and Enhancement Percentage (E) of Each Catalyst in Water.

| Sample | Concentration (wt.%) | $\bar{R}$ ($10^2$ mol·m$^{-3}$·s$^{-1}$) | m (mol/m$^3$) | E (%) |
|---|---|---|---|---|
| Water | | 38.38 | 46.05 | |
| ZnP | 0.005 | 44.77 | 53.72 | 16.65 |
| | **0.01** | 47.04 | **56.45** | **22.59** |
| | 0.03 | 45.06 | 54.07 | 17.41 |
| | 0.05 | 45.03 | 54.04 | 17.35 |
| ZnPP | 0.005 | 46.26 | 55.51 | 20.54 |
| | **0.01** | 47.29 | **56.75** | **23.24** |
| | 0.03 | 46.72 | 56.06 | 21.74 |
| | 0.05 | 46.33 | 55.59 | 20.71 |
| ZnTMPyP | 0.005 | 50.87 | 61.04 | 32.55 |
| | 0.01 | 53.83 | 64.59 | 40.26 |
| | **0.03** | 55.36 | **66.43** | **44.25** |
| | 0.05 | 51.17 | 61.40 | 33.33 |
| ZnC | 0.05 | 40.00 | 47.99 | 4.21 |
| | 0.1 | 48.18 | 57.81 | 25.54 |
| | 0.3 | 48.22 | 57.86 | 25.65 |
| | **0.5** | 49.46 | **59.35** | **28.89** |
| | 1.0 | 48.03 | 57.63 | 25.15 |

**Supplementary Table 2.** The Average $CO_2$ Absorption Rate ($\bar{R}$), Desorption Rate ($\bar{R}'$), $CO_2$ Absorption Amount (m), Desorption Amount (m′), and Enhancement Percentage of Each $K_2CO_3$ Solution (E (E′)).

| Sample | $\bar{R}$ ($\bar{R}'$) ($10^2$ mol·m$^{-3}$·s$^{-1}$) | m (m′) (mol/m$^3$) | E (E′) (%) |
|---|---|---|---|
| **Absorption stage** | **$\bar{R}$** | **m** | **E** |
| $K_2CO_3$ solution without catalyst | 20.39 | 56.08 | - |
| ZnP | 27.46 | 75.52 | 34.66 |
| ZnPP | 29.93 | 82.31 | 46.77 |
| ZnTMPyP | 28.29 | 77.81 | 38.75 |
| ZnC | 27.67 | 76.09 | 35.68 |
| **Regeneration stage** | **$\bar{R}'$** | **m′** | **E′** |
| $K_2CO_3$ solution without catalyst | 21.14 | 58.13 | - |
| ZnP | 27.01 | 74.29 | 27.80 |
| ZnPP | 29.85 | 82.10 | 41.23 |

| | | | |
|---|---|---|---|
| ZnTMPyP | 27.61 | 75.93 | 30.61 |
| ZnC | 27.03 | 74.34 | 27.87 |

**Supplementary Table 3.** Molecular Structures of Reactants during Catalytic $CO_2$ Hydration Process of Catalysts, Where Spheres of Blue, Red, Yellow, White, and Grey Respectively Represent the Atoms of Nitrogen, Oxygen, Zinc, Hydrogen, and Carbon.

| Reactant | Structure |
|---|---|
| **ZnP** | |
| P0 | 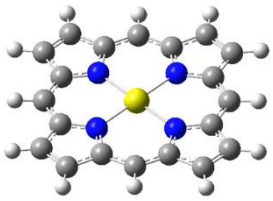 |
| P1 | 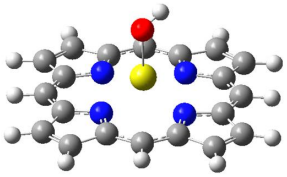 |
| P2 | 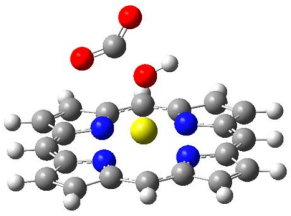 |
| P3 | 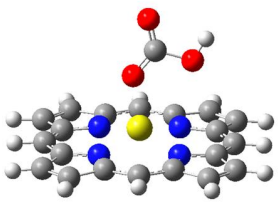 |

P4

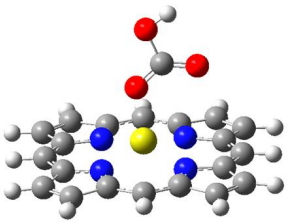

P5

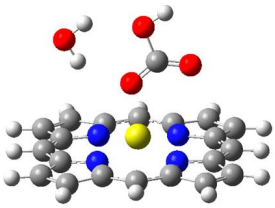

P6

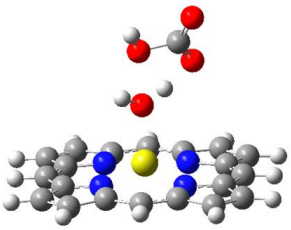

P7

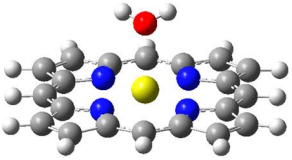

**ZnPP**

PP0

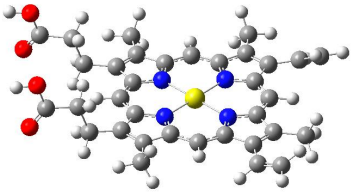

PP1

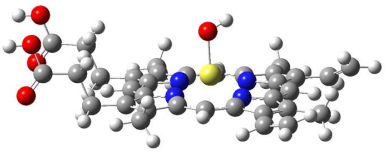

PP2

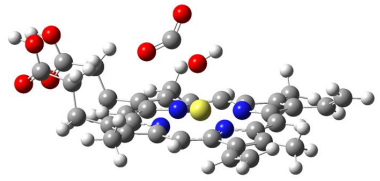

PP3

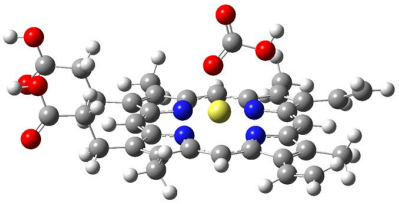

PP4

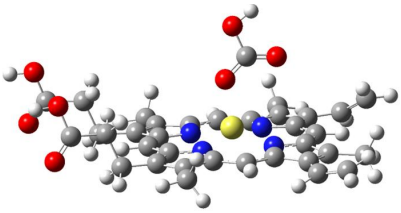

PP5

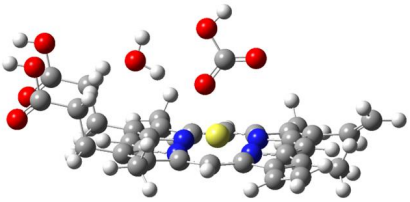

PP6

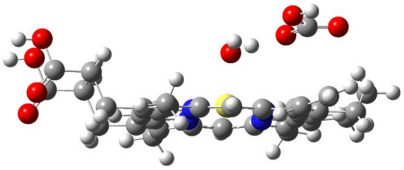

PP7

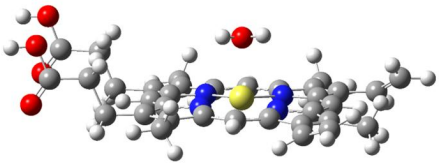

ZnTMPyP

PyP0

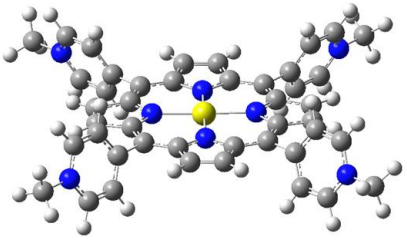

PyP1

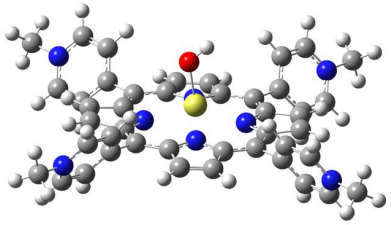

PyP2

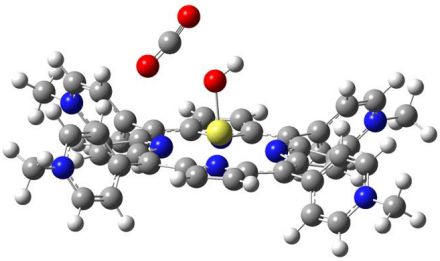

PyP3

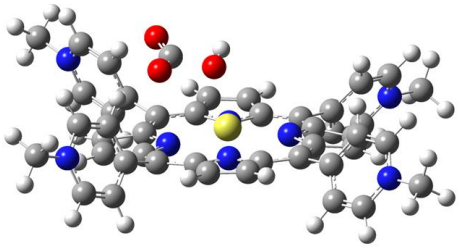

PyP4

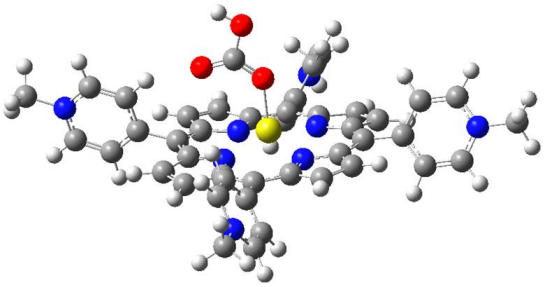

PyP5

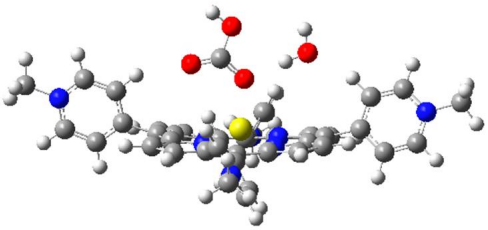

PyP6

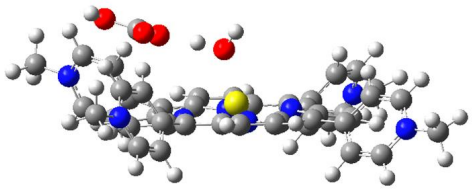

PyP7

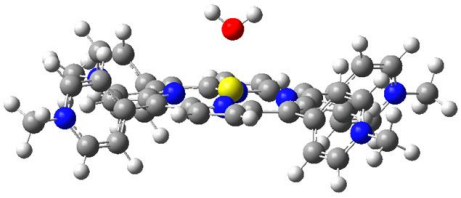

**ZnC**

C0

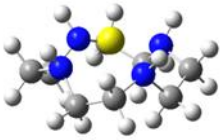

C1

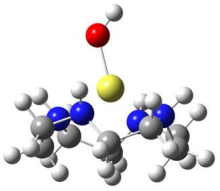

C2

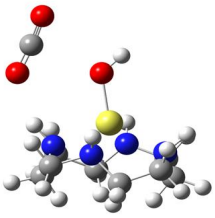

C3

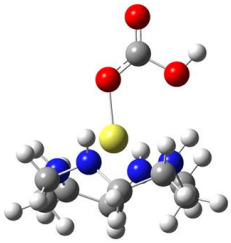

C4

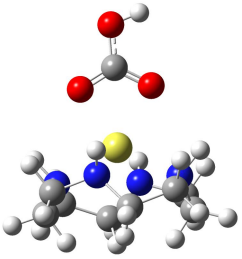

C5

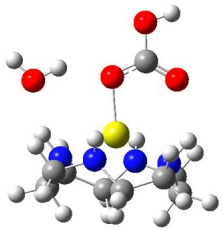

C6

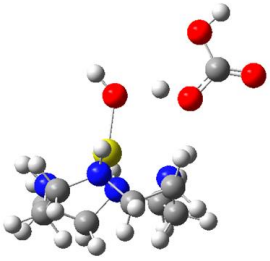

C7

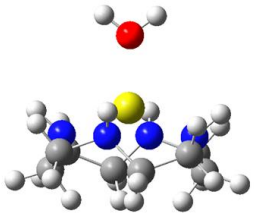

---

**Supplementary Text 1.**

**Reagents**

Pyrrole (≥99.7%), pyridine (≥99.5%), propionic acid (≥99.5%), ammonia (25% in $H_2O$), potassium carbonate ($K_2CO_3$, ≥98.0%), methanol (≥99.9%), and N, N-dimethylformamide (DMF, ≥99.9%) were obtained from Shanghai Aladdin Bio-Chem Technology Co., Ltd. (Shanghai, China). Zinc (II) acetate dihydrate (≥99.0%), 4-pyridinecarbaldehyde (≥98.0%), and anhydrous magnesium sulfate (≥98.0%) were obtained from Shanghai Bide Pharmaceutical Technology Co., Ltd. (Shanghai, China). Acetone (≥99.5%) and diethyl ether (≥98.5%) were obtained from Sinopharm Chemical Reagent Co., Ltd. (Shanghai, China). Chloroform (≥99.0%) was obtained from Nanjing Chemical Reagent Co., Ltd. (Nanjing, China). Iodomethane

(≥98.0%), formalin (18 wt. % in $H_2O$), and protoporphyrin IX (≥95.0%) were obtained from MERYER Co., Ltd. (Shanghai, China).

**Supplementary Text 2.**

**Synthesis of catalysts**

The synthetic routes of catalysts are shown in Fig.S2. Thereinto, ZnTMPyP was prepared according to the procedure in ref 1 [1] . First, meso-tetrakis(4-pyridyl) porphyrin was prepared. Pyrrole (2.5 mL, 36 mmol) and 4-pyridinecarbaldehyde (2.8 mL, 30 mmol) were added to propionic acid (100 mL) and refluxed at 141 ℃ for 2 hours. Then, the resulting solution was cooled in an ice bath, and respectively treated with acetone (400 mL) and 25% ammonia solution (100 mL), and stored in a freezer overnight. The crystallized solid was collected by filtration and washed with cold methanol. Next, the zinc [meso-tetrakis(4-pyridyl) porphyrinato] was prepared through a Zn insertion reaction. Briefly, meso-tetrakis(4-pyridyl) porphyrin and zinc acetate dihydrate (1:5 M) were dissolved in chloroform (38 mL) and the minimum amount of methanol, and stirred at room temperature for 24 h. Then, the reaction mixture was concentrated in a vacuum, and methanol was added to precipitate a solid. After filtration, the precipitate was washed with methanol and dried under a vacuum to collect a purple solid. Finally, excess iodomethane (5.2 mL, 83.27 mmol) was added to a suspension of zinc [meso-tetrakis(4-pyridyl) porphyrinato] (0.142 g, 0.208 mmol) in anhydrous DMF (20 mL) and stirred at 40 ℃ under $N_2$ atmosphere for 5 h. The resulting green solution was cooled to room temperature and diethyl ether was added to precipitate a dark green solid. The precipitate was collected by filtration and

washed with diethyl ether (0.156 g, 0.125 mmol, 60%). The solvent was removed in a vacuum and dried overnight at 80 ℃ to obtain ZnTMPyP.

The precursor of ZnP, porphin was synthesized referring to the procedure described in ref 2[2]. First, propionic acid (1 L) and pyridine (10 mL) were heated to 90 ℃ in a three-neck round bottom flask equipped with a thermometer, a reflux condenser, and an agitator. Then, under vigorous stirring, pyrrole (0.9 mL, 13 mmol) and formalin (0.9 mL, 12 mmol) were added simultaneously to the solution at 10-minute intervals. After adding a total of 13.5 mL of pyrrole and 13.5 mL of formalin, the mixture was heated for a further 60 minutes and then the air was bubbled into the hot solution over 5 minutes. The cooled solution was filtered to remove insoluble black polymers. After adding 400 mL of chloroform, the mixture was washed sequentially with water (0.8 L × 2), 1 mol/L sodium hydroxide (0.5 L × 2), and water (0.5 L × 2) to separate propionic acid. The resulting chloroform solution was filtered to eliminate remaining insoluble impurities, dehydrated by anhydrous magnesium sulfate, and then evaporated to dryness. The residue was washed with methanol until colorless, and the porphin was obtained after drying.

To prepare ZnP and ZnPP, the method for inserting $Zn^{2+}$ into ligands was the same as that for preparing ZnTMPyP.

ZnC, as the CA mimic for comparison, was prepared according to the previous literature[3].

**Supplementary Text 3.**

**Calculation on the performance parameters of the catalysts in promoting $CO_2$**

**absorption**

The performance parameters of the catalysts in promoting $CO_2$ absorption can be calculated from the absorption experiments.

Assuming that $N_2$ was not absorbed by the absorption solution, the instantaneous $CO_2$ absorption rate ($R_t$, mol/m$^3$·s$^{-1}$) in absorption solutions was calculated by:

$$R_t = \frac{y_1 - y_{2,t}}{1 - y_{2,t}} \times \frac{G_m}{V_L} \quad \text{(S1)},$$

where $y_1$ is the mole fraction of $CO_2$ in the inlet gas ($y_1$ = 0.1); $y_{2,t}$ is the mole fraction of $CO_2$ in the outlet gas at time t; $G_m$ is the mole flowrate of the inlet gas ($G_m$ = 2.98×10$^{-4}$ mol/s); and $V_L$ is the volume of absorption liquid in the bubble column ($V_L$ = 3.0×10$^{-5}$ m$^3$).

The amount of $CO_2$ absorbed (m, mol/m$^3$) by each absorption liquid over a period was calculated by:

$$m = \int_0^T R_t dt \quad \text{(S2)},$$

where T is the absorption time (120 s for water, 550 s for $K_2CO_3$ solutions for round 1, and 275 s for $K_2CO_3$ solutions for rounds 2-5).

The average $CO_2$ absorption rate ($\overline{R}$, mol/m$^3$·s$^{-1}$) in different absorption solutions was calculated by:

$$\overline{R} = \frac{m}{T} \quad \text{(S3)},$$

The enhancement percentage (E, %) was used to depict the absorption improvement by a catalyst-containing absorption liquid compared to the absorption solvent without the catalyst, and it was calculated by:

$$E = \frac{\overline{R} - \overline{R}_0}{\overline{R}_0} \times 100\% = \frac{m - m_0}{m_0} \times 100\% \quad \text{(S4)},$$

where $\overline{R}_0$ and $m_0$ are, respectively, the average $CO_2$ absorption rate and $CO_2$ absorption amount in the absorption solvent without a catalyst.

The instantaneous $CO_2$ desorption rate ($R'_t$, $mol/m^3 \cdot s^{-1}$), the average $CO_2$ desorption rate ($\overline{R'}$, $mol/m^3 \cdot s^{-1}$), the amount of $CO_2$ desorbed ($m'$, $mol/m^3$), and the enhancement percentage of $CO_2$ desorption ($E'$, **%**) during the regeneration process were calculated based on similar calculation methods to those in the absorption process.

The values of the performance parameters were taken from the average values of five absorption-desorption cycles.

**Supplementary Text 4.**

**Esterase experiment methods**

The activity assay was carried out at 2 ℃ and the temperature was maintained by ice packs. 1 mg of catalyst and 8 mL of saturated $CO_2$ solution were added into 12 mL of Tris buffer solution (pH 8.0) at 2 ℃. The period for the pH to change from 8.3 to 6.3, was recorded by a SIN-PH6.3 pH meter (Sinomeasure, China). Accordingly, the hydrase activity was determined by Eq. (S5):

$$U = 20(\frac{T_0}{T} - 1)/(mg\ catalyst) \quad \text{(S5)},$$

where U represents hydrase activity (μ = μmol $CO_2 \cdot s^{-1} mg^{-1}$); $T_0$ and T represent the time required for the pH of the reaction liquid to change from 8.3 to 6.3 without and with enzyme, respectively (s).

**Supplementary Text 5.**

**Computational methods**

Density functional theory (DFT) computations were carried out using the Gaussian 09 package of programs. The geometries were fully optimized using B3LYP functional and 6–311++G(d,p) basis set. After optimization, the energy was further computed using the M06-2X functional, def2tzvp basis set, and SMD model of solvation.

To predict the nucleophilic substitution reaction sites of each catalyst, the Fukui function of the corresponding output files of Gaussian was calculated using the Multiwfn 3.8 software [4,5] . The charge distributions of each catalyst were calculated using the atomic dipole moment corrected Hirshfeld (ADCH) population method in Multiwfn 3.8 software [6] . The interaction between the catalyst and the reactants was also calculated using Multiwfn 3.8 software combined with the IGMH (independent gradient model based on Hirshfeld partition) method[7]. The results were visualized via the VMD program to form a color-filled image[8].

**Supplementary Text 6.**

**Calculation on the $E_{ads}$, $E_{dis}$, and $pK_a$**

Firstly, the $HCO_3^-$ production rate can be assessed by the adsorption energy ($E_{ads}$) of the catalyst towards $CO_2$. The higher the $E_{ads}$ value, the faster the $HCO_3^-$ production. $E_{ads}$ can be calculated by Eq. (S6)

$$E_{ads} = E_{M-OH^- - CO_2} - \left(E_{M-OH^-} + E_{CO_2}\right) \quad \text{(S6)},$$

where $E_{DM-OH^- - CO_2}$, $E_{M-OH^-}$, and $E_{CO_2}$ represent the total energy of the $CO_2$ molecule adsorbed on the CA mimic (structure **P2**, **PP2**, **PyP2** or **C2**), the energy of the free $CO_2$ molecule, and the energy of the CA mimic bounded with $OH^-$

(structure **P1**, **PP1**, **PyP1**, or **C1**), respectively.

Secondly, the $HCO_3^-$ release rate can be evaluated by the bond-dissociation energy ($E_{dis}$) between $Zn^{2+}$ and $HCO_3^-$. The lower the $E_{dis}$ value, the easier the release of $HCO_3^-$ from the catalyst. $E_{dis}$ can be calculated by Eq. (S7)[9]

$$E_{dis} = E_{M^{2+}} + E_{H_2O} + E_{HCO_3^-} - \left(E_{M-HCO_3^-} + E_{H_2O}\right) \quad \text{(S7)},$$

where $E_{M^{2+}}$, $E_{H_2O}$, $E_{HCO_3^-}$, and $E_{M-HCO_3^-}$ represent the total energy of the free CA mimic (structure **P0**, **PP0**, **PyP0** or **C0**), free water, free $HCO_3^-$, and CA mimic bounded with $HCO_3^-$ (structure **P4**, **PP4**, **PyP4 or C4**), respectively.

Finally, the water dissociation rate can be assessed by the $pK_a$ value of the catalyst. $pK_a$, also known as the acid dissociation constant, is commonly used to assess the ability of a compound to dissociate hydrogen ions. A smaller $pK_a$ value implies a higher tendency for the catalyst to deprotonate.

$pK_a$ can be calculated by Eq. (S8)[9]

$$pK_a = 55.459 \times (l_{Zn-O}) - 94.893 \quad \text{(S8)},$$

where, $l_{Zn\text{-}O}$ refers to the bond length between the Zn and O atoms of $OH^-$ in the structure **P1** (**or PP1** or **PyP1** or **C1**), Å.

## References：


1. Larowska, D. *et al.* Graphene oxide functionalized with cationic porphyrins as materials for the photodegradation of rhodamine b. *J. Phys. Chem. C* **124**, 15769–15780 (2020).

2. Neya, S., Yodo, H. & Funasaki, N. Convenient synthesis of porphine. *J. Heterocycl. Chem* **30**, 549–550 (1993).

3. Saeed, M. & Deng, L. CO2 facilitated transport membrane promoted by mimic enzyme. *J. Memb. Sci* **494**, 196–204 (2015).

4. Lu, T. & Chen, F. Multiwfn: A multifunctional wavefunction analyzer. *J. Comput. Chem* **33**, 580–592 (2012).

5. Lu, T. & Chen, Q. Realization of conceptual density functional theory and information-theoretic approach in Multiwfn program. in *Conceptual Density Functional Theory* 631–647 (2022).

6. Lu, T. & Chen, F. Atomic dipole moment corrected Hirshfeld population method. *J. Theor. Comput. Chem* **11**, 163–183 (2012).

7. Lu, T. & Chen, Q. Independent gradient model based on Hirshfeld partition: A new method for visual study of interactions in chemical systems. *J. Comput. Chem* **43**, 539–555 (2022).

8. Humphrey, W., Dalke, A. & Schulten, K. VMD: Visual molecular dynamics. *J. Mol. Graph* **14**, 33–38 (1996).

9. Koziol, L. *et al.* Toward a small molecule, biomimetic carbonic anhydrase model: Theoretical and experimental investigations of a panel of zinc(II) aza-macrocyclic catalysts. *Inorg. Chem* **51**, 6803–6812 (2012).